HHS Public Access

Author manuscript

J Bone Miner Res. Author manuscript; available in PMC 2015 June 22.

Published in final edited form as:

J Bone Miner Res. 2014 April ; 29(4): 843–854. doi:10.1002/jbmr.2097.

RANKL Inhibitors Induce Osteonecrosis of the Jaw in Mice With Periapical Disease

Tara L Aghaloo[1], **Simon Cheong**[1], **Olga Bezouglaia**[1], **Paul Kostenuik**[2], **Elisa Atti**[1], **Sarah M Dry**[3], **Flavia Q Pirih**[4], and **Sotirios Tetradis**[1,5]

[1]Division of Diagnostic and Surgical Sciences, School of Dentistry, University of California, Los Angeles (UCLA), Los Angeles, CA, USA

[2]Amgen Inc., Thousand Oaks, CA, USA

[3]Department of Pathology and Laboratory Medicine, David Geffen School of Medicine, University of California, Los Angeles (UCLA), Los Angeles, CA, USA

[4]Section of Periodontics, School of Dentistry, University of California, Los Angeles (UCLA), Los Angeles, CA, USA

[5]Molecular Biology Institute, University of California, Los Angeles (UCLA), Los Angeles, CA, USA

Abstract

Antiresorptive medications are essential in treating diseases of pathologic osteoclastic bone resorption, including bone cancer and osteoporosis. Bisphosphonates (BPs) are the most commonly used antiresorptives in clinical practice. Although inhibition of bone resorption is important in regulating unwanted malignant and metabolic osteolysis, BP treatment is associated with potential side effects, including osteonecrosis of the jaws (ONJ). Recently, non-BP antiresorptive medications targeting osteoclastic function and differentiation, such as denosumab, have entered the clinical arena. Denosumab treatment results in a similar rate of ONJ as BPs. Animal models of ONJ, using high-dose BP treatment in combination with tooth extraction or dental disease, provide valuable tools and insight in exploring ONJ pathophysiology. However, the ability of other antiresorptives to induce ONJ-like lesions in animal models has not been explored. Such studies would be beneficial in providing support for the role of osteoclast inhibition in ONJ pathogenesis versus a direct BP effect on oral tissues. Here, we tested the ability of the receptor activator of NF-kB ligand (RANKL) inhibitors RANK-Fc (composed of the extracellular domain of RANK fused to the fragment crystallizable [Fc] portion of immunoglobulin G [IgG]) and OPG-Fc (composed of the RANKL-binding domains of osteoprotegerin [OPG] linked to the Fc portion of IgG) to induce ONJ in mice in the presence of periapical disease, but in the absence of dental extractions. We demonstrate radiographic evidence of ONJ in RANK-Fc–treated and OPG-Fc–treated mice, including inhibition of bone loss,

Address correspondence to: Sotirios Tetradis, DDS, PhD, Diagnostic and Surgical Sciences, UCLA School of Dentistry, 10833 Le Conte Ave., CHS Rm. 53-068, Los Angeles, CA 90095-1668, USA. stetradis@dentistry.ucla.edu.

Disclosures

ST has served as a paid consultant for and has received grant support from Amgen Inc. PK is a full-time employee and a shareholder of Amgen Inc. All other authors state that they have no conflicts of interest.

increased bone density, lamina dura thickening, and periosteal bone deposition. These findings closely resembled the radiographic appearance of an ONJ patient on denosumab treatment. Histologic examination revealed that RANK-Fc treatment and OPG-Fc treatment resulted in absence of osteoclasts, periosteal bone formation, empty osteocytic lacunae, osteonecrosis, and bone exposure. In conclusion, we have successfully induced ONJ in mice with periapical disease, using potent osteoclast inhibitors other than BPs. Our findings, coupled with ONJ animal models using high-dose BPs, suggest that osteoclast inhibition is pivotal to the pathogenesis of ONJ.

Keywords

PERIAPICAL DISEASE; OSTEONECROSIS OF THE JAWS; ANTIRESORPTIVES; RANK-FC; OPG-FC; MOUSE MODEL; ONJ

Introduction

Antiresorptive medications are an essential treatment for diseases of osteoclastic bone resorption, including primary and metastatic bone cancer with associated hypercalcemia, benign aggressive bone tumors, metabolic bone disorders, and osteoporosis. These medications prevent skeletal-related events, decrease tumor burden, prevent and treat bone pain, and significantly improve patients' quality of life.[1–4]

The most commonly used antiresorptives are bisphosphonates (BPs). BPs attenuate osteoclastic function by impairing osteoclastic differentiation, disrupting the cytoskeleton, decreasing intracellular transport, and inducing apoptosis.[5–7] BP effects on osteoclasts are important to the inhibition of unwanted malignant and benign osteolysis[8]; however, potential side effects including nephrotoxicity, acute flu-like symptoms, gastroesophageal irritation, atypical trochanteric femur fractures, and osteonecrosis of the jaws (ONJ) have been reported in patients on BPs.[9–12]

Osteoclasts have become the target of therapeutic strategies owing to their central role in bone diseases. Denosumab is a novel and clinically effective agent that inhibits osteoclast differentiation, function, and survival by binding to the receptor activator of NF-kB ligand (RANKL) and inhibiting its interaction with RANK on osteoclasts.[13] Clinical studies in patients with breast cancer, prostate cancer, multiple myeloma, and osteoporosis have demonstrated denosumab's ability to suppress bone turnover and skeletal-related events—similar to zoledronic acid.[14–18] However, large-scale clinical studies have also reported similar rates of ONJ in patients on denosumab or on BPs.[19–21]

ONJ is defined as exposed bone in the jaws for at least 8 weeks in patients on BPs without a history of radiation to the craniofacial region.[22,23] Although spontaneous cases have been reported, the inciting events are usually trauma, including extractions and other surgical procedures, and dental disease.[24–26] Indeed, animal tooth extraction models have been able to replicate ONJ-like lesions in mice, rats, minipigs, and dogs.[27–36] We, and others, have demonstrated that periodontal disease and a potent BP are sufficient to induce ONJ in rats.[28,29,37] Moreover, we recently developed an ONJ mouse model using high-dose BP treatment in combination with experimentally induced periapical disease (inflammation of

the tissues surrounding the apical part of the tooth root),[38] thus emphasizing the importance of dental disease in ONJ pathophysiology.

ONJ etiology and pathophysiology are still largely unknown. Several hypotheses, such as BP toxicity to the oral epithelium; altered wound healing after tooth extraction; high bone turnover of the mandible and maxilla; oral biofilm formation; infection, inflammation, and suppression of angiogenesis; and bone turnover have been proposed.[3,39] Although high-dose BPs have been tested, to the best of our knowledge, no other antiresorptives have been used to induce ONJ in animal models. Such studies would be important to provide support for the role of osteoclast inhibition in ONJ pathogenesis versus the possibility of a direct BP effect on oral tissues.[3,40] Here, we tested the ability of RANKL inhibitors to induce ONJ in mice in the presence of periapical disease, but in the absence of dental extractions.

Subjects and Methods

Animal care and experimental induction of periapical disease

Animals and surgical procedures were handled in accordance to guidelines of the UCLA Chancellor's Animal Research Committee. Thirty 16-week-old C57BL/6J male mice (Jackson Laboratories, Bar Harbor, ME, USA) were randomly divided into three groups of 10 animals that received intraperitoneal (ip) injections of either vehicle (Veh, sterile saline), 10 mg/kg mouse RANK-Fc (composed of the extracellular domain of RANK fused to the fragment crystallizable [Fc] portion of immunoglobulin G [IgG])[41] three times per week, or 10 mg/kg rat OPG-Fc (composed of the RANKL-binding domains of osteoprotegerin [OPG] linked to the Fc portion of IgG)[41,42] once per week, for 3 weeks. This injection protocol was used to account for the higher potency of OPG-Fc versus RANK-Fc in suppressing bone resorption and serum calcium levels in hypercalcemic mice.[43] RANK-Fc and OPG-Fc were provided by Amgen, Inc. (Thousand Oaks, CA, USA).

Mice were anesthetized with isoflurane and mounted on a jaw retraction board. The crowns of the right first and second mandibular molars were then drilled using a size 1/4 round burr avoiding furcal perforation, as described.[38,44,45] The crowns of the left first and second mandibular molars were kept intact. Animals continued to be treated with Veh, RANK-Fc, or OPG-Fc for an additional 9 weeks. Blood was collected via retro-orbital bleeding at the beginning of the experiment, at the time of drilling (after 3 weeks of injection), and at the end of the experiment (after 12 weeks of injection). Serum tartrate-resistant acid phosphatase 5b (TRACP5b) was measured by enzyme immunoassay (RatTRAP; JDS; Fountain Hills, AZ, USA). At the end of the experiment, animals were euthanized, mandibles were dissected, placed in 4% paraformaldehyde for 48 hours, and stored in 70% ethanol.

Micro–computed tomography scanning

Mouse mandibles were imaged by micro–computed tomography (μCT SkyScan 1172; SkyScan, Kontich, Belgium) at 10-μm resolution, and the volumetric data were converted to Digital Imaging and Communications in Medicine (DICOM) format and imported in the Dolphin Imaging software (Chatsworth, CA, USA) to generate three-dimensional (3D) and

multiplanar reconstructed images. Sagittal, coronal, and axial sections through the apical/periodontal area and 3D models of the mandibular molars were generated to quantify changes in alveolar bone structure/architecture and volume. The amount of periapical bone loss, width of the periodontal ligament (PDL) space, lamina dura thickness, lingual cortical thickness, and bone volume/tissue volume (BV/TV) were quantified as described.[38]

Histology and TRACP staining

After μCT imaging, bones were decalcified in 14.5% ethylenediaminetetraacetic acid (EDTA) solution for 3 weeks. Samples were paraffin embedded, sectioned at 5-μm-thick coronal slices along the distal root of the first molar, and hematoxylin and eosin (H&E) staining was performed. All H&E stained slides were digitally scanned using the Aperio AT automated slide scanner and the Aperio ImageScope software (Aperio Technologies, Inc., Vista, CA, USA). Using the ruler tool in ImageScope, 1 mm of the bone at the alveolar crest was marked. All measurements were performed in that area of the alveolar bone. Histologic parameters, including number of empty osteocytic lacunae, osteonecrotic area, periosteal thickness, junctional epithelium to alveolar crest distance, were quantified on the digital images as described.[38] Necrotic area was defined as loss of more than five contiguous osteocytes with confluent areas of empty lacunae. To quantify periosteal thickness, the ruler tool was used to measure the three greatest areas of both lingual and buccal periosteal thickness, which were then averaged.[38] TRAP-positive cells were identified using the leukocyte acid phosphatase kit (Sigma-Aldrich, St. Louis, MO, USA).

All histology and digital imaging was performed at the Translational Pathology Core Laboratory (TPCL) at UCLA.

ONJ patient

Panoramic and cone beam CT (CBCT) images of a patient treated with denosumab (120 mg every 4 weeks) for 24 months for control of femur giant cell tumor who developed oral bone exposure for 16 weeks, were obtained from the archives of the Oral and Maxillofacial Surgery clinic and the Oral and Maxillofacial Radiology clinic at the UCLA School of Dentistry.

Statistics

Mean and standard error of mean (SEM) were determined using Excel software formulas. Data among groups were analyzed using one-way analysis of variance (ANOVA) and statistical differences were identified by Student-Newman-Keuls multiple comparison post hoc test (GraphPad; GraphPad Software, Inc., La Jolla, CA, USA).

Results

To investigate the ability of RANK-Fc and OPG-Fc to inhibit osteoclastic function, TRACP5b serum levels were measured at the start of treatment (t1: immediately prior to the first injection), at the time of drilling (t2: after 3 weeks of injections), and at the end of the experiment (t3: after 12 weeks of injections; Fig. 1). For Veh-treated animals, serum TRACP5b levels remained similar for each time point. As expected, 3 weeks of pretreatment

with RANK-Fc or OPG-Fc significantly attenuated TRACP5b levels at the time of drilling. The TRACP5b remained at similar low levels for the duration of the experiment. All RANK-Fc–treated and OPG-Fc–treated animals showed substantial TRACP5b reduction, suggesting the successful inhibition of osteoclastic function and lack of an immunogenic response to the reagents which would lead to their rapid clearance.[46]

Sagittal μCT sections of the distal root area of the first mandibular molars (Fig. 2*A*1) were used to evaluate the periapical space (white brackets, Fig. 2*A*). Increase in the width of the periapical space was observed for the drilled site of Veh controls, indicating significant bone loss (Fig. 2*A*). RANK-Fc or OPG-Fc treatments greatly attenuated this periapical bone loss (Fig. 2*A*), which was quantified from the μCT reconstructions (Fig. 2*B*).

Sagittal μCT sections through the furcation area of mandibular molars in Veh-treated animals demonstrated normal lamina dura thickness (thick arrow, Fig. 3*A*) and PDL space width (thin arrow, Fig. 3*A*). At the drilled site of the same mice, bone loss and widening of the PDL space (thin arrows, Fig. 3*A*) and loss of lamina dura in part of the furcation area were noted. In contrast, the RANK-Fc–treated and OPG-Fc–treated mice appeared to show preservation of the PDL space (thin arrows, Fig. 3*A*) with thickening of the lamina dura (thick arrows, Fig. 3*A*) at the furcation area of drilled teeth. Quantification on the μCT images confirmed a statistically significant increase in PDL space and decrease in lamina dura thickness at the furcation of drilled teeth in Veh-treated animals. Antiresorptive treatment caused a significant and dramatic inhibition of PDL space widening. PDL space for RANK-Fc was not statistically different, and for OPG-Fc it was mildly increased compared to the non-drilled teeth (Fig. 3*B*). A statistically significant decrease in lamina dura thickness was seen at the apex of drilled compared to healthy teeth in Veh-treated mice. RANK-Fc and OPG-Fc treatment reversed this effect and resulted in a statistically significant increase of lamina dura thickness compared to healthy teeth in all groups (Fig. 3*C*). Interestingly, RANK-Fc but not OPG-Fc treatment caused a moderate statistically significant increase in lamina dura thickness in the furcation of healthy teeth relative to healthy teeth of Veh-treated mice (Fig. 3*C*).

Axial slices through the alveolar ridge showed significant osteolysis in the drilled versus the healthy site of Veh-treated animals (thin arrows, Fig. 4*A*). In contrast, bone integrity was preserved in healthy and drilled sites of both RANK-Fc–treated and OPG-Fc–treated animals. Interestingly, new bone deposition on the buccal and lingual periosteal surfaces of the alveolar ridge was observed on the drilled side of RANK-Fc–treated and OPG-Fc–treated mice (thick arrows, Fig. 4*A*). Periosteal bone deposition was observed on the drilled site of all RANK-Fc–treated and OPG-Fc–treated mice (Table 1).

To quantify the effect of periapical disease on alveolar bone structure, the lingual cortical thickness was measured. Periapical disease significantly reduced cortical thickness in the drilled site of Veh-treated animals. RANK-Fc and OPG-Fc treatment statistically increased cortical thickness in the healthy side of the mandible. Periapical disease in the same animals caused a further significant increase in cortical thickness (Fig. 4*B*). Periapical disease in control mice caused a significant decrease in BV/TV, suggesting overall alveolar bone loss.

In contrast, periapical disease in mice on antiresorptive treatment reversed and even significantly increased BV/TV of the alveolar ridge (Fig. 4*C*).

The radiographic changes observed in mice on antiresorptive treatment closely resembled radiographic findings seen in ONJ patients on denosumab (XGEVA; Amgen Inc.) treatment. Figure 5 presents the panoramic (Fig. 5*A*) and select CBCT coronal (Fig. 5*B*), sagittal (Fig. 5*C*), and axial (Fig. 5*D*) sections of such a patient with bone exposure at the left retromolar area. White thick arrows point to periosteal bone deposition, white thin arrows to increased lamina dura thickness, black thick arrows to increased trabecular density, black thin arrow to widened periapical space, and black-and-white arrow to periodontal bone loss at the distal surface of the left second mandibular molar. The patient had no history of tooth extraction prior to the clinical bone exposure.

Histologic evaluation indicated that non-drilled teeth in all treatment groups had normal alveolar bone and marginal epithelium (yellow and red arrows, respectively; Fig. 6*A*, *A*1, *C*, *C*1, *E*, *E*1). Drilled teeth in all groups showed inflammatory infiltrate of gingival tissues (white arrows, Fig. 6*B*, *D*, *F*). Reduction of the alveolar crest height and increase of the distance between the marginal epithelium and the alveolar crest was observed at the drilled teeth of Veh-treated animals (Fig. 6*B*, *B*1, yellow and double-headed black arrows). The alveolar crest height was preserved around drilled teeth of RANK-Fc–treated and OPG-Fc–treated mice and this resulted in preservation of the marginal epithelium to alveolar crest distance (Fig. 6*D*, *D*1, *F*, *F*1, yellow and double-headed black arrows). Importantly, areas of empty osteocytic lacunae indicating necrotic bone, as well as periosteal bone formation were seen in the drilled site of all RANK-Fc and OPG-Fc animals (Fig. 6*D*, *D*1, *F*, *F*1, black and blue arrows; Table 1). In 2 Veh-treated animals, small osteonecrotic areas were present (Table 1). In 2 RANK-Fc–treated and 3 OPG-Fc–treated mice, areas of exposed bone were also present (Table 1; Fig. 6*D*, *D*1, *F*, *F*1 green arrows).

To evaluate the ability of RANK-Fc and OPG-Fc to inhibit osteoclast differentiation and function within the mandible, TRAP staining was performed (Fig. 7*A*). Few TRAP+ cells were present in the healthy site of Veh-treated animals. Periapical disease resulted in high numbers of TRAP+ cells in the same animals. Near complete absence of osteoclasts was observed in the healthy or drilled site of RANK-Fc–treated and OPG-Fc–treated sites (Fig. 7*B*).

Quantification of histologic findings revealed increased thickness of periosteum on the drilled versus healthy site for all treatment groups. RANK-Fc and OPG-Fc versus Veh increased periosteal thickness of the alveolar bone around non-drilled teeth. Importantly, both RANK-Fc and OPG-Fc treatment induced a significantly increased thickness of periosteum on the drilled site compared to Veh treatment (Fig. 8*A*).

The junctional epithelium to alveolar crest distance also was assessed (Fig. 8*B*). Drilled teeth showed a significantly increased distance compared to healthy teeth in the Veh-treated mice, suggesting increased resorption of the alveolar crest. RANK-Fc and OPG-Fc treatment significantly inhibited the epithelium to alveolar crest distance in the drilled site. The

epithelium to crest distance in the RANK-Fc–treated and OPG-Fc–treated animals was not different between healthy versus drilled sites.

The number of empty osteocytic lacunae and the size of osteonecrotic area were evaluated at the area of the alveolar ridge in the healthy and drilled sites (Fig. 8*C, D*). RANK-Fc and OPG-Fc caused a statistically significant increase both in empty osteocytic lacunae and in the area of osteonecrosis compared to the healthy site of the same animals, as well as compared to the healthy and drilled sites of Veh-treated animals. The OPG-Fc treatment effect was mildly but statistically lower compared to the RANK-Fc effect. The osteonecrotic areas covered on average 25.8% for RANK-Fc and 17.7% for OPG-Fc and measured 203,543 ± 31,756 μm^2 for RANK-Fc and 129,235 ± 17,651 μm^2 for OPG-Fc. The osteonecrotic areas in the 2 Veh-treated animals covered 6.5% and measured 32,401 ± 2461 μm^2. We also measured the percent osteonecrotic area in a 50-μm zone adjacent to the periosteal bone deposition in RANK-Fc–treated and OPG-Fc–treated animals. Indeed, a significantly higher osteonecrosis area was observed adjacent to periosteal bone (PB) deposits compared to the percent osteonecrotic area for the total alveolar bone (TB) (Fig. 8*E*).

Discussion

ONJ is a well-known and difficult to manage complication of antiresorptive therapy, which can result in pain, infection, bone sequestration, tooth loss, intraoral and extraoral fistulae, and jaw fracture.[25,47] ONJ was first reported a decade ago in patients with bone malignancy or osteoporosis. Since then, many studies have attempted to elucidate the pathophysiology of ONJ.[1,24,47] Animal models, in which trauma from tooth extraction, periodontal disease, vitamin D deficiency, immunosuppression, and chemotherapy have led to ONJ-like lesions in mice, rats, and minipigs treated with high-dose BPs have had a significant impact in addressing the disease pathogenesis of BPs.[27–35] Potent BPs are the common factor in all of these animal models. Whether suppression of bone remodeling is the only BP mechanism or whether other cellular or tissue effects of BPs contribute to ONJ development remains controversial.[1,40] The availability of other antiresorptive medications that have pharmacologic actions distinct from BPs, but that nonetheless are associated with ONJ in patients, provide another opportunity to study the effects of bone remodeling suppression on the development of ONJ.

In this study, we provide the first radiographic and histologic evidence that treatment with RANKL inhibitors in combination with periapical disease induces ONJ-like lesions in mice, a finding that supports the theory that suppression of bone remodeling is a critical step for ONJ formation. RANK-Fc and OPG-Fc treatment attenuated bone loss associated with periapical disease; increased alveolar bone density, lamina dura thickness, and periosteal bone deposition; caused osteonecrosis (characterized by the presence of empty osteocytic lacunae); and induced bone exposure. Importantly, changes in alveolar bone morphology in RANK-Fc–treated and OPG-Fc–treated mice resembled the appearance of alveolar bone in an ONJ patient on denosumab treatment. In this ONJ animal model, bone exposure was detected histologically at the area of the alveolar crest adjacent to the molar teeth. Because we did not perform tooth extractions, no large areas of alveolar bone exposure were created.

Although we closely examined the alveolar ridge using a dissecting microscope for obvious uncovered bone, we did not explore small areas of exposure under debris, to avoid artificially altering tissue relationships.

RANKL is an important protein for osteoclastogenesis that is expressed by many cell types, including osteoblasts; stromal, dendritic, synovial, periodontal ligament; B cells; some tumor cells; fibroblasts; odontoblasts; cementoblasts; ameloblasts; and activated lymphocytes.[48–55] RANKL knockout mice demonstrate decreased osteoclast numbers, defective bone remodeling, severe osteopetrosis, and no tooth eruption.[56,57] RANKL binding to RANK induces osteoclast differentiation and function.[58–60] RANK activation initiates signaling pathways that mediate osteoclastogenesis and induce osteoclast function through expression of osteoclastic genes such as cathepsin K, TRAP, and matrix metalloproteinases.[61,62]

A central player in the regulation of the RANKL-RANK system is OPG,[42,58,63] a secreted glycoprotein produced by osteoblasts, endothelial cells, fibroblasts, dendritic cells, bone marrow stromal cells, B-lymphocytes, chondrocytes, and smooth muscle cells.[48,52,58,61] OPG functions as a decoy receptor for RANKL, preventing the RANKL-RANK interaction.[58,64] The ratio of available RANKL versus OPG is a critical determinant in RANK signaling and in osteoclast differentiation and function. Mice and rats overexpressing OPG demonstrate increased bone density, decreased marrow spaces, and decreased bone resorption.[65,66] Increased RANKL and decreased OPG expression resulting in an augmented RANKL/OPG ratio have been reported in periodontal and periapical lesions in experimental animal models and patients.[67–70] Attenuation of osteoclastic activity decreases bone loss induced by experimental periodontal[71–73] or periapical[74] disease and has been considered a possible treatment intervention in patients.[75]

Because of its importance in osteoclastogenesis and bone remodeling, RANKL-RANK-OPG signaling has been targeted to manage bone disorders.[76,77] Denosumab is a fully-human monoclonal antibody that binds soluble and membrane-bound human RANKL with high affinity, and interrupts RANKL-RANK interaction with a resulting decrease in osteoclast numbers, decrease in serum markers of bone turnover, increase in bone mass and density, and decrease in tumor-induced osteolysis.[41,42,78–80] Denosumab is U.S. Food and Drug Administration (FDA)-approved to treat postmenopausal women with osteoporosis, to increase bone mass in men with nonmetastatic prostate cancer on high-dose androgen-deprivation therapy, and in women with breast cancer on aromatase therapy, all of whom are at high risk for fracture. Denosumab is also approved for preventing skeletal-related events in patients with bone metastases from solid tumors.[42] Further ongoing clinical trials are using denosumab to treat men with osteoporosis, to prevent or delay bone metastases in breast and prostate cancer, and to treat giant cell tumor.[42,81]

Denosumab recognizes human and monkey, but not mouse or rat RANKL,[37] so other recombinant RANKL inhibitors such as RANK-Fc and OPG-Fc have been used to inhibit RANKL in animal models.[46,82–86] In this study, RANKL was inhibited by RANK-Fc or OPG-Fc, using dosing regimens intended to maximally inhibit osteoclasts throughout the 12-week treatment period. RANK-Fc binds RANKL and potently inhibits bone resorption in

preclinical models.[41] OPG-Fc similarly binds RANKL; increases bone density and bone volume in mouse, rat, and monkey models; decreases osteoclast number; and increases biomechanical strength after ovariectomy.[41,42] Indeed, in our experiments, RANK-Fc and OPG-Fc significantly inhibited TRACP5b in serum, illustrating successful systemic osteoclast inhibition. This was achieved at the time of experimental periapical disease induction, and was sustained until the end of the experiment.

In our studies, most of the time RANK-Fc and OPG-Fc were equally effective in attenuating osteoclastic activity and producing radiographic and histologic ONJ-like changes in mice. Comparable effects of RANK-Fc and OPG-Fc have also been reported for attenuation of bone resorption during *Staphylococcus aureus*–induced arthritis.[87] RANK-Fc, like denosumab, binds only RANKL, whereas OPG can also recognize the tumor necrosis factor (TNF)-related apoptosis-inducing ligand (TRAIL), which shares a 25% amino acid sequence homology with RANKL.[88,89] The nearly similar ability of RANK-Fc and OPG-Fc to induce ONJ-like lesions in our studies points to the central involvement of the RANKL-RANK signaling cascade in disease pathophysiology.

Moderate but statistically significant differences in periosteal thickness, empty osteocytic lacunae, and osteonecrotic area were seen, in which RANK-Fc induced a higher increase compared to OPG-Fc. The treatment protocol of the animals most probably underlies these differences. In our experiments, RANK-Fc was injected three times per week, whereas OPG-Fc was injected one time per week. Consequently, RANK-Fc could have resulted in a more sustained osteoclast inhibition. Alternatively, the effects of OPG-Fc could have been modified owing to its activity of recognizing TRAIL.[89] TRAIL-activation of transmembrane TRAIL receptors (TRAIL-Rs) induces apoptosis in a variety of cells. Osteoclasts express TRAIL-R, and TRAIL-induced osteoclastic apoptosis has been reported.[90] Thus, the effectiveness of OPG in inhibiting osteoclast differentiation and function could be partially counteracted by inhibition of osteoclast apoptosis through attenuation of TRAIL signaling.[89]

The RANK-Fc and OPG-Fc effects in the present study were qualitatively and quantitatively similar to each other and to changes we recently reported using high-dose zoledronic acid treatment of mice in the presence of periapical disease.[38] An interesting difference between the two studies was the near complete absence of TRAP+ cells in the alveolar bone of healthy and diseased sites in RANK-Fc–treated and OPG-Fc–treated mice. This is in contrast to the increased number of TRAP+ cells with altered morphology in the diseased site of BP-treated mice.[38] The difference in osteoclast appearance reflects the distinct pharmacologic mode of action to inhibit bone resorption between BPs versus RANK-Fc or OPG-Fc. Whereas BPs target mature osteoclasts, actively resorbing bone to induce their apoptosis, RANK-Fc and OPG-Fc target osteoclast differentiation, thus significantly decreasing the number of osteoclasts.[13] The overall similarities of ONJ-like features associated with BPs versus RANKL inhibitors might also indicate that dysfunctional osteoclasts which might persist in BP-treated patients are not critical to ONJ etiology.

An additional difference between our previous study using BP treatment[38] and our present findings was the presence of a small but statistically significant increase of empty osteocytic

lacunae in the healthy mandible of zoledronic acid–treated animals that was not observed with RANK-Fc or OPG-Fc treatment. Similar findings of mandible areas lacking viable osteocytes and void of patent canaliculi have been reported in dogs treated with oral alendronate for 1 to 3 years.[91] The increase of empty osteocytic lacunae with BP treatment but not with RANK-Fc or OPG-Fc treatment suggests that in addition to suppression of bone remodeling, BPs might have direct toxic effects that induce osteocyte death.

In 2 Veh-treated animals, small areas of osteonecrosis were observed. This finding was unexpected; the reason for the development of osteonecrosis in the absence of antiresorptive treatment is not clear. In our previous study using the same animal model of periapical disease,[38] no osteonecrotic areas were seen in the Veh-treated animals. Furthermore, the literature does not report osteonecrosis in control animals when this well-established model of experimental periapical disease is used. Potentially, the presence of small osteonecrotic areas in the control group could represent an uncommon response of bone to severe inflammation, because other researchers have reported necrotic bone as a result of infection or mechanical trauma in the jaws of patients not receiving antiresorptives.[92,93]

In conclusion, we present a mouse model of non-BP antiresorptive-induced ONJ with radiographic and histologic features similar to human ONJ. To the best of our knowledge, this is the first ONJ animal model that used antiresorptive treatment other than BPs. Collectively, our results, in combination with investigations of BP-induced ONJ in various animal models and settings, and with ONJ patient studies, strongly support the central importance of osteoclast inhibition in ONJ pathophysiology.

Acknowledgments

This work was supported by grants from Amgen Inc., NIH/NIDCR DE019465, and by minority supplement DE 019465-S1. We acknowledge Marina Stolina and Chun-Ya Han for measurement of serum TRACP5b.

Authors' roles: All authors participated in the design, execution, and analyses of the studies. TA, SC, and ST drafted the manuscript. All authors made revisions to the manuscript and approved the final version.

References

1. Allen MR. Bisphosphonates and osteonecrosis of the jaw: moving from the bedside to the bench. Cells Tissues Organs. 2009; 189(1–4):289–94. [PubMed: 18698128]
2. Clezardin P. Anti-tumour activity of zoledronic acid. Cancer Treat Rev. 2005; 31(Suppl 3):1–8. [PubMed: 16225995]
3. Landesberg R, Woo V, Cremers S, et al. Potential pathophysiological mechanisms in osteonecrosis of the jaw. Ann N Y Acad Sci. 2011; 1218:62–79. [PubMed: 21291478]
4. Roelofs AJ, Thompson K, Gordon S, Rogers MJ. Molecular mechanisms of action of bisphosphonates: current status. Clin Cancer Res. 2006; 12(20 Pt 2):6222s–30s. [PubMed: 17062705]
5. Kimmel DB. Mechanism of action, pharmacokinetic and pharmaco-dynamic profile, and clinical applications of nitrogen-containing bisphosphonates. J Dent Res. 2007; 86(11):1022–33. [PubMed: 17959891]
6. Ito M, Amizuka N, Nakajima T, Ozawa H. Ultrastructural and cytochemical studies on cell death of osteoclasts induced by bisphosphonate treatment. Bone. 1999; 25(4):447–52. [PubMed: 10511111]
7. Suzuki K, Takeyama S, Sakai Y, Yamada S, Shinoda H. Current topics in pharmacological research on bone metabolism: inhibitory effects of bisphosphonates on the differentiation and activity of osteoclasts. J Pharmacol Sci. 2006; 100(3):189–94. [PubMed: 16518076]

8. Shipman CM, Rogers MJ, Apperley JF, Russell RG, Croucher PI. Bisphosphonates induce apoptosis in human myeloma cell lines: a novel anti-tumour activity. Br J Haematol. 1997; 98(3):665–72. [PubMed: 9332325]

9. Lewiecki EM. Safety of long-term bisphosphonate therapy for the management of osteoporosis. Drugs. 2011; 71(6):791–814. [PubMed: 21504254]

10. Orozco C, Maalouf NM. Safety of bisphosphonates. Rheum Dis Clin North Am. 2012; 38(4):681–705. [PubMed: 23137577]

11. Saleh A, Hegde VV, Potty AG, Lane JM. Bisphosphonate therapy and atypical fractures. Orthop Clin North Am. 2013; 44(2):137–51. [PubMed: 23544820]

12. Watts NB, Diab DL. Long-term use of bisphosphonates in osteoporosis. J Clin Endocrinol Metab. 2010; 95(4):1555–65. [PubMed: 20173017]

13. Baron R, Ferrari S, Russell RG. Denosumab and bisphosphonates: different mechanisms of action and effects. Bone. 2011; 48(4):677–92. [PubMed: 21145999]

14. Stopeck AT, Lipton A, Body JJ, et al. Denosumab compared with zoledronic acid for the treatment of bone metastases in patients with advanced breast cancer: a randomized, double-blind study. J Clin Oncol. 2010; 28(35):5132–9. [PubMed: 21060033]

15. Fizazi K, Carducci M, Smith M, et al. Denosumab versus zoledronic acid for treatment of bone metastases in men with castration-resistant prostate cancer: a randomised, double-blind study. Lancet. 2011; 377(9768):813–22. [PubMed: 21353695]

16. Henry DH, Costa L, Goldwasser F, et al. Randomized, double-blind study of denosumab versus zoledronic acid in the treatment of bone metastases in patients with advanced cancer (excluding breast and prostate cancer) or multiple myeloma. J Clin Oncol. 2011; 29(9):1125–32. [PubMed: 21343556]

17. Cummings SR, San Martin J, McClung MR, et al. Denosumab for prevention of fractures in postmenopausal women with osteoporosis. N Engl J Med. 2009; 361(8):756–65. [PubMed: 19671655]

18. Keaveny T, McClung M, Genant H, et al. Femoral and vertebral strength improvements in postmenopausal women with osteoporosis treated with denosumab. J Bone Miner Res. Epub 2013 Jun;21. DOI: 10.1002/jbmr.2024.

19. Smith MR, Saad F, Coleman R, et al. Denosumab and bone-metastasis-free survival in men with castration-resistant prostate cancer: results of a phase 3, randomised, placebo-controlled trial. Lancet. 2012; 379(9810):39–46. [PubMed: 22093187]

20. Saad F, Brown JE, Van Poznak C, et al. Incidence, risk factors, and outcomes of osteonecrosis of the jaw: integrated analysis from three blinded active-controlled phase III trials in cancer patients with bone metastases. Ann Oncol. 2012; 23(5):1341–7. [PubMed: 21986094]

21. Dranitsaris G, Hatzimichael E. Interpreting results from oncology clinical trials: a comparison of denosumab to zoledronic acid for the prevention of skeletal-related events in cancer patients. Support Care Cancer. 2012; 20(7):1353–60. [PubMed: 22539050]

22. Ruggiero SL, Dodson TB, Assael LA, Landesberg R, Marx RE, Mehrotra B. American Association of Oral and Maxillofacial Surgeons position paper on bisphosphonate-related osteonecrosis of the jaws—2009 update. J Oral Maxillofac Surg. 2009; 67(5 Suppl):2–12. [PubMed: 19371809]

23. Khosla S, Burr D, Cauley J, et al. Bisphosphonate-associated osteonecrosis of the jaw: report of a task force of the American Society for Bone and Mineral Research. J Bone Miner Res. 2007; 22(10):1479–91. [PubMed: 17663640]

24. Marx RE. Pamidronate (Aredia) and zoledronate (Zometa) induced avascular necrosis of the jaws: a growing epidemic. J Oral Maxillofac Surg. 2003; 61(9):1115–7. [PubMed: 12966493]

25. Marx RE, Sawatari Y, Fortin M, Broumand V. Bisphosphonate-induced exposed bone (osteonecrosis/osteopetrosis) of the jaws: risk factors, recognition, prevention, and treatment. J Oral Maxillofac Surg. 2005; 63(11):1567–75. [PubMed: 16243172]

26. Migliorati CA, Schubert MM, Peterson DE, Seneda LM. Bisphospho-nate-associated osteonecrosis of mandibular and maxillary bone: an emerging oral complication of supportive cancer therapy. Cancer. 2005; 104(1):83–93. [PubMed: 15929121]

27. Abtahi J, Agholme F, Sandberg O, Aspenberg P. Bisphosphonate-induced osteonecrosis of the jaw in a rat model arises first after the bone has become exposed. No primary necrosis in unexposed bone. J Oral Pathol Med. 2012; 41(6):494–9. [PubMed: 22268631]
28. Aghaloo TL, Kang B, Sung EC, et al. Periodontal disease and bisphosphonates induce osteonecrosis of the jaws in the rat. J Bone Miner Res. 2011; 26(8):1871–82. [PubMed: 21351151]
29. Aguirre JI, Akhter MP, Kimmel DB, et al. Oncologic doses of zoledronic acid induce osteonecrosis of the jaw-like lesions in rice rats (Oryzomys palustris) with periodontitis. J Bone Miner Res. 2012; 27(10):2130–43. [PubMed: 22623376]
30. Ali-Erdem M, Burak-Cankaya A, Cemil-Isler S, et al. Extraction socket healing in rats treated with bisphosphonate: animal model for bisphosphonate related osteonecrosis of jaws in multiple myeloma patients. Med Oral Patol Oral Cir Bucal. 2011; 16(7):e879–3. [PubMed: 21743422]
31. Bi Y, Gao Y, Ehirchiou D, et al. Bisphosphonates cause osteonecrosis of the jaw-like disease in mice. Am J Pathol. 2010; 177(1):280–90. [PubMed: 20472893]
32. Lopez-Jornet P, Camacho-Alonso F, Molina-Minano F, Gomez-Garcia F, Vicente-Ortega V. An experimental study of bisphosphonate-induced jaws osteonecrosis in Sprague-Dawley rats. J Oral Pathol Med. 2010; 39(9):697–702. [PubMed: 20819131]
33. Kikuiri T, Kim I, Yamaza T, et al. Cell-based immunotherapy with mesenchymal stem cells cures bisphosphonate-related osteonecrosis of the jaw-like disease in mice. J Bone Miner Res. 2010; 25(7):1668–79. [PubMed: 20200952]
34. Sonis ST, Watkins BA, Lyng GD, Lerman MA, Anderson KC. Bony changes in the jaws of rats treated with zoledronic acid and dexamethasone before dental extractions mimic bisphosphonate-related osteonecrosis in cancer patients. Oral Oncol. 2009; 45(2):164–72. [PubMed: 18715819]
35. Pautke C, Kreutzer K, Weitz J, et al. Bisphosphonate related osteonecrosis of the jaw: a minipig large animal model. Bone. 2012; 51(3):592–9. [PubMed: 22575441]
36. Allen MR, Chu TM, Ruggiero SL. Absence of exposed bone following dental extraction in beagle dogs treated with 9 months of high-dose zoledronic acid combined with dexamethasone. J Oral Maxillofac Surg. Jun; 2013 71(6):1017–26. [PubMed: 23375897]
37. Gotcher JE, Jee WS. The progress of the periodontal syndrome in the rice cat. II. The effects of a diphosphonate on the periodontium. J Periodontal Res. 1981; 16(4):441–55. [PubMed: 6459441]
38. Kang B, Cheong S, Chaichanasakul T, et al. Periapical disease and bisphosphonates induce osteonecrosis of the jaws in mice. J Bone Miner Res. 2013; 28(7):1631–40. [PubMed: 23426919]
39. Yamashita J, McCauley LK. Antiresorptives and osteonecrosis of the jaw. J Evid Based Dent Pract. 2012; 12(3 Suppl):233–47. [PubMed: 23040351]
40. Allen MR, Burr DB. The pathogenesis of bisphosphonate-related osteonecrosis of the jaw: so many hypotheses, so few data. J Oral Maxillofac Surg. 2009; 67(5 Suppl):61–70. [PubMed: 19371816]
41. Kostenuik PJ, Nguyen HQ, McCabe J, et al. Denosumab, a fully human monoclonal antibody to RANKL, inhibits bone resorption and increases BMD in knock-in mice that express chimeric (murine/human) RANKL. J Bone Miner Res. 2009; 24(2):182–95. [PubMed: 19016581]
42. Lacey DL, Boyle WJ, Simonet WS, et al. Bench to bedside: elucidation of the OPG-RANK-RANKL pathway and the development of denosumab. Nat Rev Drug Discov. 2012; 11(5):401–19. [PubMed: 22543469]
43. Miller RE, Branstetter D, Armstrong A, et al. Receptor activator of NF-kappa B ligand inhibition suppresses bone resorption and hypercalcemia but does not affect host immune responses to influenza infection. J Immunol. 2007; 179(1):266–74. [PubMed: 17579046]
44. Wang CY, Stashenko P. Kinetics of bone-resorbing activity in developing periapical lesions. J Dent Res. 1991; 70(10):1362–6. [PubMed: 1939830]
45. Sasaki H, Hou L, Belani A, et al. IL-10, but not IL-4, suppresses infection-stimulated bone resorption in vivo. J Immunol. 2000; 165(7):3626–30. [PubMed: 11034365]
46. Ominsky MS, Li X, Asuncion FJ, et al. RANKL inhibition with osteoprotegerin increases bone strength by improving cortical and trabecular bone architecture in ovariectomized rats. J Bone Miner Res. 2008; 23(5):672–82. [PubMed: 18433301]

47. Ruggiero SL, Mehrotra B, Rosenberg TJ, Engroff SL. Osteonecrosis of the jaws associated with the use of bisphosphonates: a review of 63 cases. J Oral Maxillofac Surg. 2004; 62(5):527–34. [PubMed: 15122554]
48. Boyce BF, Xing L. Functions of RANKL/RANK/OPG in bone modeling and remodeling. Arch Biochem Biophys. 2008; 473(2):139–46. [PubMed: 18395508]
49. Fukushima H, Kajiya H, Takada K, Okamoto F, Okabe K. Expression and role of RANKL in periodontal ligament cells during physiological root-resorption in human deciduous teeth. Eur J Oral Sci. 2003; 111(4):346–52. [PubMed: 12887401]
50. Han S, Koo J, Bae J, Kim S, Baik S, Kim MY. Modulation of TNFSF expression in lymphoid tissue inducer cells by dendritic cells activated with Toll-like receptor ligands. BMB Rep. 2011; 44(2):129–34. [PubMed: 21345313]
51. Josien R, Wong BR, Li HL, Steinman RM, Choi Y. TRANCE, a TNF family member, is differentially expressed on T cell subsets and induces cytokine production in dendritic cells. J Immunol. 1999; 162(5):2562–8. [PubMed: 10072496]
52. Tat SK, Pelletier JP, Velasco CR, Padrines M, Martel-Pelletier J. New perspective in osteoarthritis: the OPG and RANKL system as a potential therapeutic target? Keio J Med. 2009; 58(1):29–40. [PubMed: 19398882]
53. Teng YT, Nguyen H, Gao X, et al. Functional human T-cell immunity and osteoprotegerin ligand control alveolar bone destruction in periodontal infection. J Clin Invest. 2000; 106(6):R59–67. [PubMed: 10995794]
54. Wang Z, McCauley LK. Osteoclasts and odontoclasts: signaling pathways to development and disease. Oral Dis. 2011; 17(2):129–42. [PubMed: 20659257]
55. Yasuda H, Shima N, Nakagawa N, et al. Osteoclast differentiation factor is a ligand for osteoprotegerin/osteoclastogenesis-inhibitory factor,is identical to TRANCE/RANKL. Proc Natl Acad Sci U S.A. 1998; 95(7):3597–602. [PubMed: 9520411]
56. Kim N, Odgren PR, Kim DK, Marks SC Jr, Choi Y. Diverse roles of the tumor necrosis factor family member TRANCE in skeletal physiology revealed by TRANCE deficiency and partial rescue by a lymphocyte-expressed TRANCE transgene. Proc Natl Acad Sci U S A. 2000; 97(20): 10905–10. [PubMed: 10984520]
57. Kong YY, Yoshida H, Sarosi I, et al. OPGL is a key regulator of osteoclastogenesis, lymphocyte development and lymph-node organogenesis. Nature. 1999; 397(6717):315–23. [PubMed: 9950424]
58. Reid P, Holen I. Pathophysiological roles of osteoprotegerin (OPG). Eur J Cell Biol. 2009; 88(1): 1–17. [PubMed: 18707795]
59. Tsurukai T, Udagawa N, Matsuzaki K, Takahashi N, Suda T. Roles of macrophage-colony stimulating factor and osteoclast differentiation factor in osteoclastogenesis. J Bone Miner Metab. 2000; 18(4):177–84. [PubMed: 10874596]
60. Udagawa N, Takahashi N, Yasuda H, et al. Osteoprotegerin produced by osteoblasts is an important regulator in osteoclast development and function. Endocrinology. 2000; 141(9):3478–84. [PubMed: 10965921]
61. Silva I, Branco JC. RANK/RANKL/OPG: literature review. Acta Reumatol Port. 2011; 36(3):209–18. [PubMed: 22113597]
62. Edwards JR, Mundy GR. Advances in osteoclast biology: old findings and new insights from mouse models. Nat Rev Rheumatol. 2011; 7(4):235–43. [PubMed: 21386794]
63. Nakashima T, Hayashi M, Takayanagi H. New insights into osteoclastogenic signaling mechanisms. Trends Endocrinol Metab. 2012; 23(11):582–90. [PubMed: 22705116]
64. Simonet WS, Lacey DL, Dunstan CR, et al. Osteoprotegerin: a novel secreted protein involved in the regulation of bone density. Cell. 1997; 89(2):309–19. [PubMed: 9108485]
65. Stolina M, Dwyer D, Ominsky MS, et al. Continuous RANKL inhibition in osteoprotegerin transgenic mice and rats suppresses bone resorption without impairing lymphorganogenesis or functional immune responses. J Immunol. 2007; 179(11):7497–505. [PubMed: 18025194]
66. Ominsky MS, Stolina M, Li X, et al. One year of transgenic overexpression of osteoprotegerin in rats suppressed bone resorption and increased vertebral bone volume, density, and strength. J Bone Miner Res. 2009; 24(7):1234–46. [PubMed: 19257823]

67. Belibasakis GN, Rechenberg DK, Zehnder M. The receptor activator of NF-kappaB ligand-osteoprotegerin system in pulpal and periapical disease. Int Endod J. 2013; 46(2):99–111. [PubMed: 22900632]
68. Kawashima N, Suzuki N, Yang G, et al. Kinetics of RANKL, RANK and OPG expressions in experimentally induced rat periapical lesions. Oral Surg Oral Med Oral Pathol Oral Radiol Endod. 2007; 103(5):707–11. [PubMed: 17336108]
69. Crotti T, Smith MD, Hirsch R, et al. Receptor activator NF kappaB ligand (RANKL) and osteoprotegerin (OPG) protein expression in periodontitis. J Periodontal Res. 2003; 38(4):380–7. [PubMed: 12828654]
70. Mogi M, Otogoto J, Ota N, Togari A. Differential expression of RANKL and osteoprotegerin in gingival crevicular fluid of patients with periodontitis. J Dent Res. 2004; 83(2):166–9. [PubMed: 14742657]
71. Han X, Lin X, Yu X, et al. Porphyromonas gingivalis infection-associated periodontal bone resorption is dependent on receptor activator of NF-kappaB ligand. Infect Immun. 2013; 81(5): 1502–9. [PubMed: 23439308]
72. Yuan H, Gupte R, Zelkha S, Amar S. Receptor activator of nuclear factor kappa B ligand antagonists inhibit tissue inflammation and bone loss in experimental periodontitis. J Clin Periodontol. 2011; 38(11):1029–36. [PubMed: 22092474]
73. Jin Q, Cirelli JA, Park CH, et al. RANKL inhibition through osteoprotegerin blocks bone loss in experimental periodontitis. J Periodontol. 2007; 78(7):1300–8. [PubMed: 17608585]
74. Xiong H, Wei L, Hu Y, Zhang C, Peng B. Effect of alendronate on alveolar bone resorption and angiogenesis in rats with experimental periapical lesions. Int Endod J. 2010; 43(6):485–91. [PubMed: 20536576]
75. Badran Z, Kraehenmann MA, Guicheux J, Soueidan A. Bisphosphonates in periodontal treatment: a review. Oral Health Prev Dent. 2009; 7(1):3–12. [PubMed: 19408809]
76. Hofbauer LC, Neubauer A, Heufelder AE. Receptor activator of nuclear factor-kappaB ligand and osteoprotegerin: potential implications for the pathogenesis and treatment of malignant bone diseases. Cancer. 2001; 92(3):460–70. [PubMed: 11505389]
77. Kostenuik PJ, Shalhoub V. Osteoprotegerin: a physiological and pharmacological inhibitor of bone resorption. Curr Pharm Des. 2001; 7(8):613–35. [PubMed: 11375772]
78. Bekker PJ, Holloway DL, Rasmussen AS, et al. A single-dose placebo-controlled study of AMG 162, a fully human monoclonal antibody to RANKL, in postmenopausal women. J Bone Miner Res. 2004; 19(7):1059–66. [PubMed: 15176987]
79. Kostenuik PJ, Smith SY, Jolette J, Schroeder J, Pyrah I, Ominsky MS. Decreased bone remodeling and porosity are associated with improved bone strength in ovariectomized cynomolgus monkeys treated with denosumab, a fully human RANKL antibody. Bone. 2011; 49(2):151–61. [PubMed: 21457806]
80. Ominsky MS, Stouch B, Schroeder J, et al. Denosumab, a fully human RANKL antibody, reduced bone turnover markers and increased trabecular and cortical bone mass, density, and strength in ovariectomized cynomolgus monkeys. Bone. 2011; 49(2):162–73. [PubMed: 21497676]
81. Thomas D, Henshaw R, Skubitz K, et al. Denosumab in patients with giant-cell tumour of bone: an open-label, phase 2 study. Lancet Oncol. 2010; 11(3):275–80. [PubMed: 20149736]
82. Akiyama T, Dass CR, Shinoda Y, Kawano H, Tanaka S, Choong PF. Systemic RANK-Fc protein therapy is efficacious against primary osteosarcoma growth in a murine model via activity against osteoclasts. J Pharm Pharmacol. 2010; 62(4):470–6. [PubMed: 20604836]
83. Cho SW, Sun HJ, Yang JY, et al. Transplantation of mesenchymal stem cells overexpressing RANK-Fc or CXCR4 prevents bone loss in ovariectomized mice. Mol Ther. 2009; 17(11):1979–87. [PubMed: 19603006]
84. Sordillo EM, Pearse RN. RANK-Fc: a therapeutic antagonist for RANK-L in myeloma. Cancer. 2003; 97(3 Suppl):802–12. [PubMed: 12548579]
85. Li X, Ominsky MS, Stolina M, et al. Increased RANK ligand in bone marrow of orchiectomized rats and prevention of their bone loss by the RANK ligand inhibitor osteoprotegerin. Bone. 2009; 45(4):669–76. [PubMed: 19539794]

86. Bargman R, Posham R, Boskey A, et al. High- and low-dose OPG-Fc cause osteopetrosis-like changes in infant mice. Pediatr Res. 2012; 72(5):495–501. [PubMed: 22926546]

87. Verdrengh M, Bokarewa M, Ohlsson C, Stolina M, Tarkowski A. RANKL-targeted therapy inhibits bone resorption in experimental Staphylococcus aureus-induced arthritis. Bone. 2010; 46(3):752–8. [PubMed: 19879986]

88. Zauli G, Secchiero P. The role of the TRAIL/TRAIL receptors system in hematopoiesis and endothelial cell biology. Cytokine Growth Factor Rev. 2006; 17(4):245–57. [PubMed: 16750931]

89. Zauli G, Melloni E, Capitani S, Secchiero P. Role of full-length osteoprotegerin in tumor cell biology. Cell Mol Life Sci. 2009; 66(5):841–51. [PubMed: 19011755]

90. Chamoux E, Houde N, L'Eriger K, Roux S. Osteoprotegerin decreases human osteoclast apoptosis by inhibiting the TRAIL pathway. J Cell Physiol. 2008; 216(2):536–42. [PubMed: 18338379]

91. Burr DB, Allen MR. Mandibular necrosis in beagle dogs treated with bisphosphonates. Orthod Craniofac Res. 2009; 12(3):221–8. [PubMed: 19627524]

92. Farah CS, Savage NW. Oral ulceration with bone sequestration. Aust Dent J. 2003; 48(1):61–4. [PubMed: 14640160]

93. Meer S, Coleman H, Altini M, Alexander T. Mandibular osteomyelitis and tooth exfoliation following zoster-CMV co-infection. Oral Surg Oral Med Oral Pathol Oral Radiol Endod. 2006; 101(1):70–5. [PubMed: 16360610]

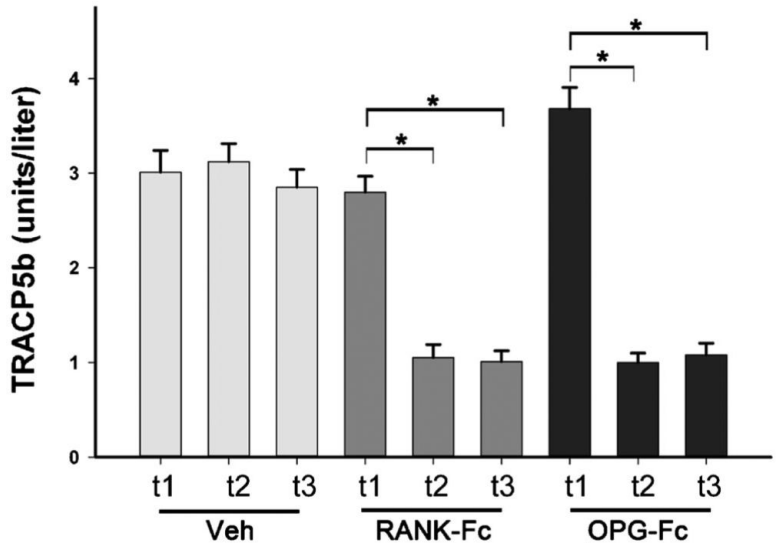

Fig. 1.

TRACP5b serum levels were measured at the beginning (t1), at the time of drilling (t2), and at the end of the experiment (t3) for animals treated with Veh, RANK-Fc or OPG-Fc. *Statistically significantly different, $p < 0.001$. TRACP = tartrate-resistant acid phosphatase; Veh = vehicle; RANK = receptor activator of NF-kB; Fc = fragment crystallizable; IgG = immunoglobulin G; RANK-Fc = extracellular domain of RANK fused to the Fc portion of IgG; OPG = osteoprotegerin; RANKL = RANK ligand; OPG-Fc = RANKL-binding domains of OPG linked to the Fc portion of IgG.

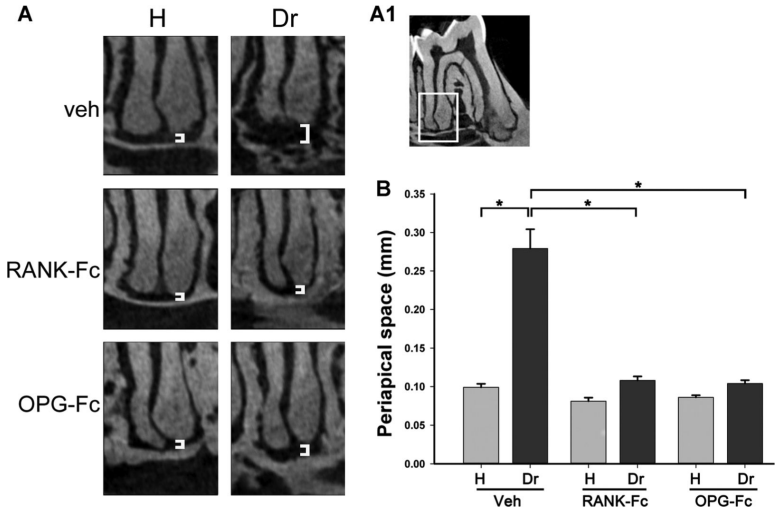

Fig. 2.

Changes in the periapical area of molars from animals treated with Veh, RANK-Fc, or OPG-Fc. (*A*) μCT images of the periapical area of the first molar distal root of healthy and drilled sites in animals treated with Veh, RANK-Fc, or OPG-Fc. (*A*1) The periapical area of the first molar distal root, as depicted in *A*. (*B*) Quantification of periapical space at the distal root of the first molar. *Statistically significantly different, $p < 0.001$. Veh = vehicle; RANK = receptor activator of NF-kB; Fc = fragment crystallizable; IgG = immunoglobulin G; RANK-Fc = extracellular domain of RANK fused to the Fc portion of IgG; OPG = osteoprotegerin; RANKL = RANK ligand; OPG-Fc = RANKL-binding domains of OPG linked to the Fc portion of IgG; μCT = micro–computed tomography.

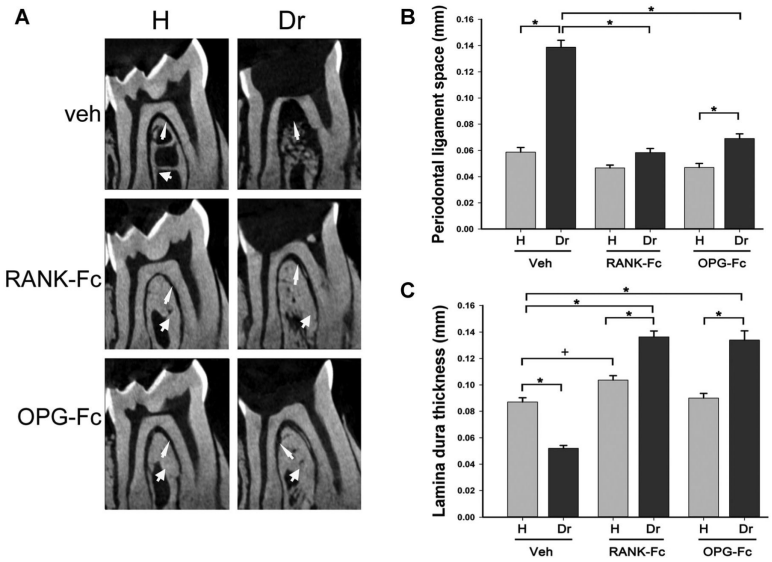

Fig. 3.

Changes in the furcational area of molars from mice treated with Veh, RANK-Fc, or OPG-Fc. (*A*) μCT images of the furcation area of the first molar of healthy and drilled sites in mice treated with Veh, RANK-Fc, or OPG-Fc. Thin arrows point to the PDL space and thick arrows point to the lamina dura. (*B*) The PDL space width and (*C*) lamina dura thickness at the furcation area were quantified for all animal groups. *Statistically significantly different, $p < 0.001$. +Statistically significantly different, $p < 0.05$. Veh = vehicle; RANK = receptor activator of NF-kB; Fc = fragment crystallizable; IgG = immunoglobulin G; RANK-Fc = extracellular domain of RANK fused to the Fc portion of IgG; OPG = osteoprotegerin; RANKL = RANK ligand; OPG-Fc = RANKL-binding domains of OPG linked to the Fc portion of IgG; μCT = micro–computed tomography; PDL = periodontal ligament.

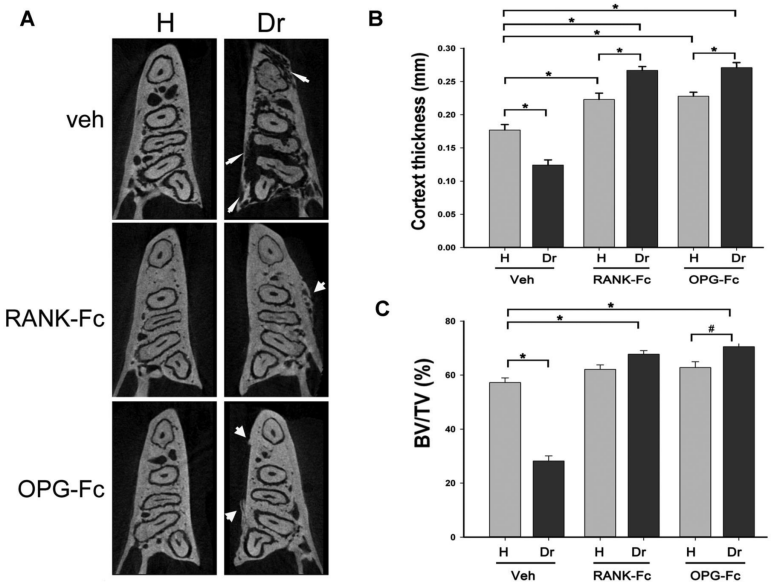

Fig. 4.

Changes in alveolar bone architecture in animals treated with Veh, RANK-Fc, or OPG-Fc. (*A*) Axial μCT slices of the alveolar ridge at molar root level are shown. Thin arrows point to osteolysis extending to the mandibular cortices seen in the drilled site of the Veh-treated animals. Thick arrows point to periosteal bone formation and increased trabecular density seen in RANK-Fc–treated or OPG-Fc–treated animals. (*B*) Lingual cortex thickness at the distal root of the first molar and (*C*) BV/TV of bone at the area of the alveolar ridge were measured. *Statistically significantly different, $p < 0.001$, #Statistically significantly different, $p < 0.01$. Veh = vehicle; RANK = receptor activator of NF-kB; Fc = fragment crystallizable; IgG = immunoglobulin G; RANK-Fc = extracellular domain of RANK fused to the Fc portion of IgG; OPG = osteoprotegerin; RANKL = RANK ligand; OPG-Fc = RANKL-binding domains of OPG linked to the Fc portion of IgG; μCT = micro–computed tomography; BV/TV = bone volume/tissue volume.

Fig. 5.

Panoramic (*A*), coronal (*B*), sagittal (*C*), and axial (*D*) CBCT sections through the left mandibular alveolar ridge of a patient with ONJ treated with denosumab. Thin white arrows point to the thickened lamina dura, thick white arrows to periosteal bone deposition, thin black arrow to widened periapical PDL space, thick black arrows to increased bone density, and black and white arrow to loss of periodontal bone at the distal surface of the second left mandibular molar. CBCT = cone beam computed tomography; ONJ = osteonecrosis of the jaws; PDL = periodontal ligament.

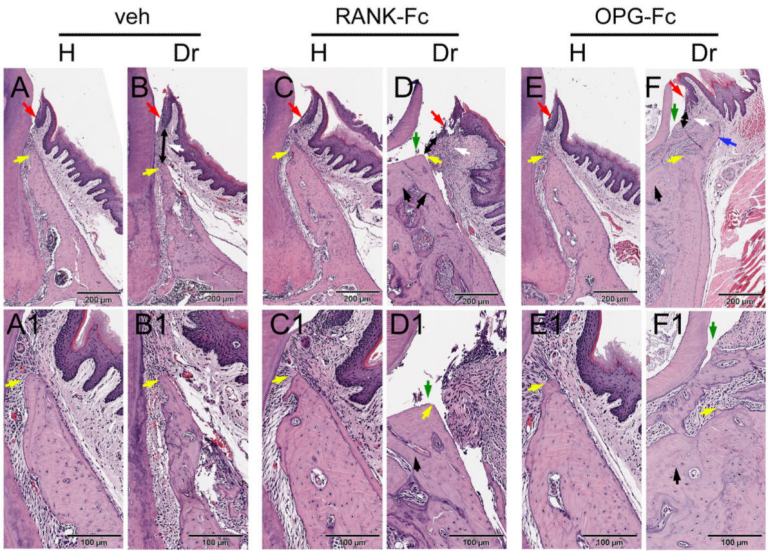

Fig. 6.

Histology of periodontal and alveolar bone area. (*A*, *A*1) Healthy site of a Veh-treated animal. (*B*, *B*1) Drilled site of a Veh-treated animal. (*C*, *C*1) Healthy site of a RANK-Fc–treated animal. (*D*, *D*1) Drilled site of a RANK-Fc–treated animal. (*E*, *E*1) Healthy site of an OPG-Fc–treated animal. (*F*, *F*1) Drilled site of an OPG-Fc–treated animal. *A*, *B*, *C*, *D*, *E*, and *F* are at × 4 magnification; *A*1, *B*1, *C*1, *D*1, *E*1, and *F*1 at × 10 magnification. Red arrows point to marginal gingival epithelium, yellow arrows to the crestal alveolar bone, white arrows to inflammatory infiltrate, black double-headed arrows to the epithelialcrestal bone distance, black arrows to areas of osteonecrosis, blue arrows to periosteal bone deposition, and green arrows to areas of exposed bone. Veh = vehicle; RANK = receptor activator of NF-kB; Fc = fragment crystallizable; IgG = immunoglobulin G; RANK-Fc = extracellular domain of RANK fused to the Fc portion of IgG; OPG = osteoprotegerin; RANKL = RANK ligand; OPG-Fc = RANKL-binding domains of OPG linked to the Fc portion of IgG.

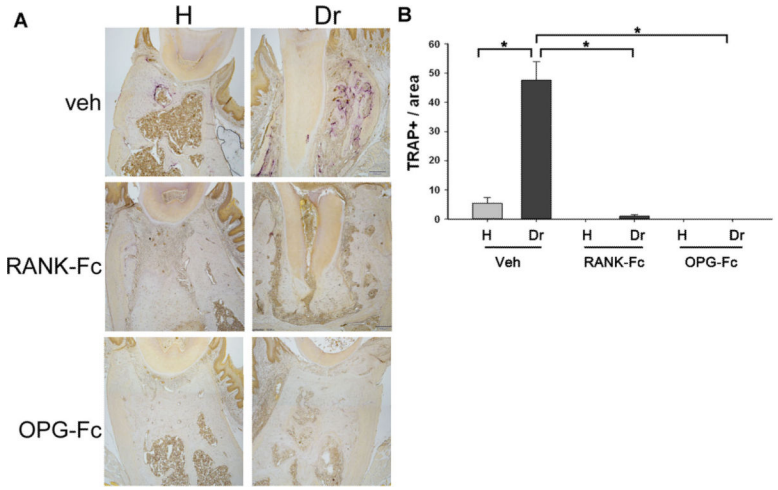

Fig. 7.

(*A*) TRAP staining on histologic sections from the alveolar ridge of healthy and drilled sites from Veh-treated, RANK-Fc–treated, and OPG-Fc–treated animals. (*B*) Number of TRAP+ cells in the healthy and drilled site of Veh-treated and BP-treated animals. *Statistically significantly different, $p < 0.001$. TRAP = Tartrate-resistant acid phosphatase; Veh = vehicle; RANK = receptor activator of NF-kB; Fc = fragment crystallizable; IgG = immunoglobulin G; RANK-Fc = extracellular domain of RANK fused to the Fc portion of IgG; OPG = osteoprotegerin; RANKL = RANK ligand; OPG-Fc = RANKL-binding domains of OPG linked to the Fc portion of IgG; BP = bisphosphonate.

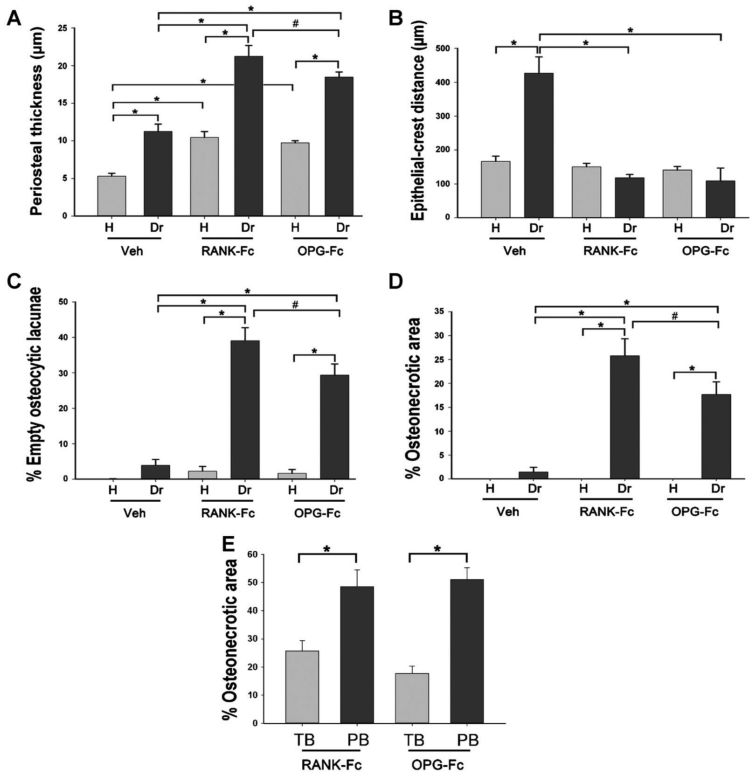

Fig. 8.

Quantification of histologic findings in the healthy and drilled site of Veh-treated, RANK-Fc–treated and OPG-Fc–treated animals. (*A*) Periosteal thickness. (*B*) The shortest epithelial-crest distance was determined. If epithelium extended below the level of the alveolar crest, a negative value was assigned to the measurement. (*C*) Percent empty osteocytic lacunae. (*D*) Percent osteonecrotic area. (*E*) The TB and percent osteonecrotic area in a 50-μm-wide band adjacent to PB were measured. *Statistically significantly different, $p < 0.001$. #Statistically significantly different, $p < 0.01$. Veh = vehicle; RANK = receptor activator of NF-kB; Fc = fragment crystallizable; IgG = immunoglobulin G; RANK-Fc = extracellular domain of RANK fused to the Fc portion of IgG; OPG = osteoprotegerin; RANKL = RANK ligand; OPG-Fc = RANKL-binding domains of OPG linked to the Fc portion of IgG; TB = total bone percent osteonecrotic area; PB = periosteal bone.

Table 1

Radiographic and Histologic Findings in Mice Treated With Veh, RANK-Fc, or OPG-Fc

Treatment	Mice (*n*)	Periosteal bone formation	Histologic osteonecrosis	Bone exposure
Veh	10	0 (0)	2 (20)	0 (0)
RANK-Fc	10	10 (100)	10 (100)	2 (20)
OPG-Fc	10	10 (100)	10 (100)	3 (30)

Values are *n* (%).

Veh = vehicle; RANK = receptor activator of NF-κB; Fc = fragment crystallizable; IgG = immunoglobulin G; RANK-Fc = extracellular domain of RANK fused to the Fc portion of IgG; OPG = osteoprotegerin; RANKL = RANK ligand; OPG-Fc = RANKL-binding domains of OPG linked to the Fc portion of IgG.